

Synthesis of the Oil-Based Nanoblocker Poly(MMA–BMA–BA–St) and the Study of the Blocking Mechanism

Daqi Li, Xianguang Wang, Yu Chen, Zixuan Han, and Gang Xie*

Cite This: *ACS Omega* 2022, 7, 40799–40806

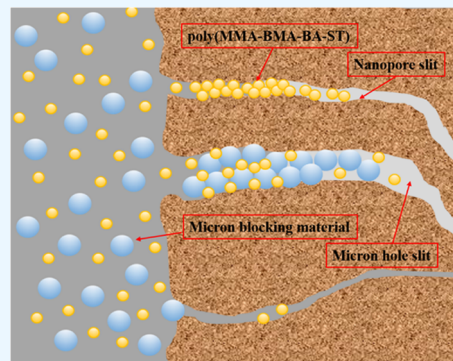
Read Online

ACCESS |

Metrics & More

Article Recommendations

ABSTRACT: Well wall instability is one of the problems that seriously affect the efficiency of oil and gas drilling and extraction, and the economic losses caused by accidents due to well wall instability amount to billions of dollars every year. Aiming at the fact that well wall stabilization is the current technical difficulty of drilling shale gas horizontal wells with oil-based drilling fluids, the oil-based nanoplugging agent poly(MMA–BMA–BA–St) was synthesized by the Michael addition reaction with compounds such as styrene, methyl methacrylate, and butyl methacrylate as raw materials. The structure and characteristics of the oil-based nanoblocker poly(MMA–BMA–BA–St) were characterized by infrared spectroscopy, particle size analysis, and thermal weight loss analysis. The particle size distribution of poly(MMA–BMA–BA–St) is 80.56–206.61 nm, with an average particle size of 137.10 nm, and it can resist the high temperature of 372 °C. The effects of poly(MMA–BMA–BA–St) on the performance parameters of oil-based drilling fluids were investigated by rheological experiments, electrical stability tests, and HTHP filtration loss experiments. The results show that when poly(MMA–BMA–BA–St) is added at 0.5 wt %, it has less influence on the rheological parameters of drilling fluids, the breaking emulsion pressure remains basically unchanged, the stability of the drilling fluid is better, the dynamic-plastic ratio of the drilling fluid is higher than 0.27, the filtration loss is the lowest, and it shows good rock-carrying properties. The results of mud cake experiments and artificial lithology experiments show that poly(MMA–BMA–BA–St) has the best sealing effect, with a mud cake permeability of 1.12×10^{-4} mD and a sealing rate of 30.00% when added at 0.5 wt %; the artificial core permeability was 4.0×10^{-4} mD, and the sealing rate was 91.23%. Poly(MMA–BMA–BA–St) showed good sealing performance. The oil-based nanoplugging agent poly(MMA–BMA–BA–St) has good dispersion in oil-based drilling fluids and can enter the nanopore joints to form a dense plugging layer under the action of formation pressure to prevent the intrusion of drilling fluids, thus reducing the impact of drilling fluids on the formation, maintaining the stability of the well wall and reducing downhole complications.



1. INTRODUCTION

With the depletion of conventional natural gas, shale gas, as an important unconventional gas, is receiving increasing attention.^{1,2} Shale gas exploration and development, mainly in the Sichuan basin, will be the main force for future shale gas production growth in China.^{3–6} The shale reservoir is characterized by low permeability and strong adsorption, and microfractures are developed, the formation is easily fractured, and the clay mineral content is high and water-sensitive.^{7,8} Oil-based drilling fluids are natural inhibitors. Oil-based drilling fluids are highly resistant to contamination and have good lubricity, so they are commonly used for drilling long horizontal section shale gas wells.^{9,10} As the complexity of drilling encountered formations increases, oil-based drilling fluids can still lead to severe well wall collapse for hard, brittle, and fractured formations with developed laminae and microfractures,^{11–14} despite their natural inhibition, due to the fact that the intrusion of filtrate can easily make the formation unstable, in addition to the transmission of hydraulic pressure through microfractures, which can also lead to well wall

destabilization.^{15–19} Therefore, it is the focus of scholars' research to strengthen the oil-based drilling fluid to seal the nanoporous seam, improve the stability of the well wall, and maintain the stable performance of the drilling fluid.^{20,21}

Research on oil-based drilling fluid sealants has yielded some results. Xie et al. synthesized hyperbranched polyamines with a particle size of 36.7 nm and good thermal stability to seal nanopore joints in shale formations.²² Geng et al. used oleic acid as a surface modifier to reduce the surface free energy of surface-modified nanoscale polystyrene (NS) and improve its dispersion stability in mineral oil. NS can withstand temperatures up to 252 °C. The addition of 2 wt % NS to the base

Received: May 21, 2022

Accepted: October 14, 2022

Published: November 2, 2022



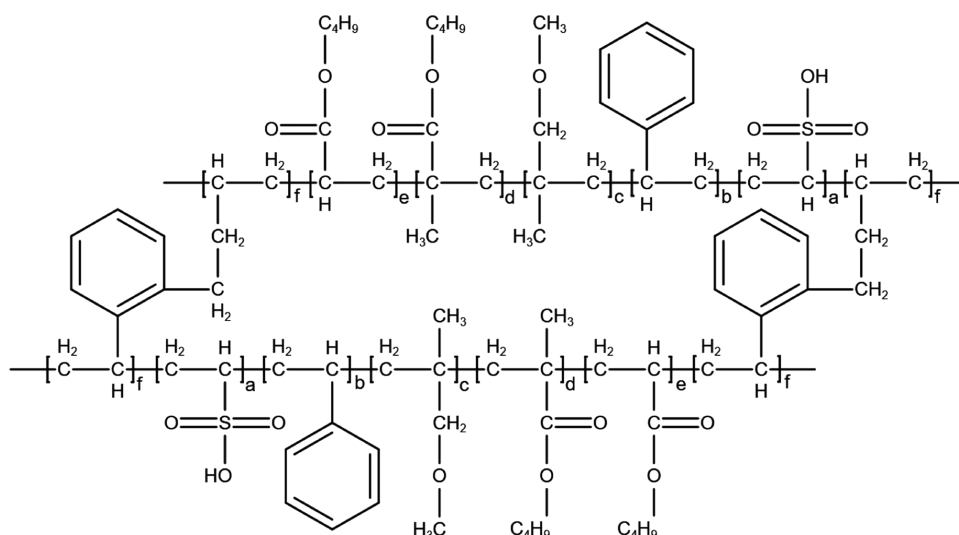


Figure 1. Chemical structure formula of poly(MMA–BMA–BA–St).

slurry resulted in a 67% reduction in the filtration loss of the permeation plugging device compared to the base slurry without NS addition, and in the pressure transfer test, the downstream pressure did not change significantly after 60 h, showing a good sealing effect.²³ Li et al. synthesized butylbenzene resin/silica nanoparticle (SBR/SiO₂) composites by continuous emulsion polymerization. SBR/SiO₂ can be dispersed in both water and mineral oil with a temperature resistance of 352 °C and an average particle size of 62.4 nm in the aqueous phase and 265.1 nm in the oil phase. SBR/SiO₂ can enter into the nanopores of shale formations and significantly reduce fluid intrusion, thus improving wellbore stability.²⁴ Li et al. synthesized polymer nanospheres (PNS) with a double cross-linked structure for well wall destabilization; the average particle size of PNS is 133 nm, and the initial decomposition temperature is about 315 °C, which can effectively seal the shale pore space.²⁵ However, the blocking agent has a large impact on the rheological performance of the drilling fluid, and it is difficult to meet the technical requirements of the drilling fluid for performance.²⁶ Li et al. prepared a new nanopolymer emulsion NPE with good environmental protection and excellent plugging performance by emulsion polymerization technology for the problem of the large particle size of the traditional drilling fluid blocking agent, which is difficult to effectively seal the micropores and microfractures of shale. The particle size of the emulsion is kept between 75 and 240 nm, with good high-temperature stability, which can effectively seal shale micropores and microfractures, reduce shale permeability, and improve shale well wall stability.²⁷ All of the above-mentioned nanoplugging materials have shown good plugging effects in laboratory studies, but there are also disadvantages, such as insufficient temperature resistance of nanoplugging materials, complicated synthesis, and high addition, which has a large impact on the performance of drilling fluids and cannot be widely used.

Compared with conventional oil-based rigid plugging materials, nanoflexible materials have the characteristics of small particle size and deformability, which can not only enter nanofractures under pressure but also be used in combination with rigid bridging particles to fill nanopores and form a dense plugging layer. In this paper, poly(MMA–BMA–BA–St), an oil-based nanosealing material, was synthesized by the Michael

addition reaction using styrene,²⁷ methyl methacrylate, butyl methacrylate, and other compounds as monomers and raw materials. Poly(MMA–BMA–BA–St) can enter the nanopore fracture to form a seal and can also be used in combination with large-size rigid sealing materials to improve the sealing performance of drilling fluids. The structure of poly(MMA–BMA–BA–St) contains hydrophobic groups such as ester groups, which enable it to be uniformly dispersed in oil-based drilling fluids, and it contains a benzene ring with high-temperature resistance, which makes poly(MMA–BMA–BA–St) have strong temperature resistance. Poly(MMA–BMA–BA–St) is added in small amounts in drilling fluids, which has less impact on the performance of oil-based drilling fluids. Therefore, poly(MMA–BMA–BA–St) can be used as a plugging agent in oil-based drilling fluids.

2. EXPERIMENTAL METHODS

2.1. Materials and Instruments. Sodium dodecyl sulfate, sodium vinyl sulfate, styrene (St), methyl methacrylate (MMA), butyl methacrylate (BMA), divinylbenzene (DVB), butyl acrylate (BA), and ammonium persulfate (APS) are from Chengdu Kelong Chemical Reagent Factory; 3# white oil, CaCl₂, main emulsifier, auxiliary emulsifier, wetting agent, filter loss reducing agent, organic soil, quicklime, and barite are all industrial products.

The high-temperature and high-pressure filter loss meter (GGS42-2A) is from Shandong Qingdao Haitongda Special Instrument Co.; 6700 is from Thermolectric Corporation; the laser scattering system (BI-200SM) is from Brookhaven Instruments; and the simultaneous thermal analyzer (TGA/DSC1) is from METTLER, Switzerland.

2.2. Preparation of Nanomaterials. A small amount of sodium dodecyl sulfate and sodium vinyl sulfonate was weighed into a three-necked flask with a capacity of 500 mL, ultrapure water was added to dissolve, the temperature was raised to 40 °C, the mixture was stirred until dispersion, and nitrogen gas was passed to react for 3 h. The temperature of the solution was raised to 45 °C, and styrene, methyl methacrylate, butyl methacrylate, butyl acrylate, and divinylbenzene were slowly added dropwise using a constant pressure-dropping funnel. The 500 mL capacity of the three-necked flask was placed in a constant temperature water bath

and heated to the reaction temperature. The nitrogen gas was passed, and the mixture was stirred for 1 h at 300 rpm. After the reaction was complete, it was left to stand for 20 min, and a small amount of ultrapure water containing ammonium sulfate was added slowly dropwise using a constant pressure-dropping funnel, warmed to 65 °C, and reacted for 10 h under the condition of passing nitrogen to obtain poly(MMA–BMA–BA–St). The chemical structure formula of poly(MMA–BMA–BA–St) is shown in Figure 1.

2.3. Permeability Calculation Formula. **2.3.1. Mud Cake Experiment.** The base drilling fluid was prepared according to the oil-based drilling fluid formula (80% 3# white oil + 20% CaCl₂ brine with 25% concentration + 0.6% primary emulsifier + 1.5% secondary emulsifier + 0.8% wetting agent + 3% organic soil + 3% quicklime + 8% filter loss reducing agent + several barite). Different volume fraction additions of plugging materials were added to the base drilling fluid, the mixture stirred at high speed, and then a plugging evaluation test was conducted on a Type 42 high-temperature and high-pressure water loss meter.

The permeability of the mud cake is calculated by eq 1,

$$K = \frac{100Q\mu L}{A\Delta P} \quad (1)$$

where K is the permeability of the “artificial mud cake,” mD; Q is the average volume of water loss per second, cm³/s; μ is the viscosity of the filtrate, mPa·s; L is the thickness (or length) of the mud cake, cm; A is the area of the filter cake, cm²; and ΔP is the filter loss differential pressure, MPa. Here the area of the filter cake = 23.8 cm²; filter loss pressure difference = 3.5 MPa.

2.3.2. Artificial Core Experiments. Poly(MMA–BMA–BA–St) corresponding to the lowest permeability value obtained in the mud cake experiment was added to 3# white oil in a spiked amount to prepare 300 mL of the mixed liquid solution. The mixture was stirred for 30 min and then ultrasonically dispersed for 30 min at a temperature of 50 °C. The mixed solutions of 3# white oil and 3# white oil + the optimum amount of poly(MMA–BMA–BA–St) were added to the SCMS-C4 high-temperature and high-pressure dense core permeability testing device, and the artificial core experiments were conducted at 110 °C and a differential pressure of 3.5 MPa. The permeability was calculated by eq 1.

2.3.3. Evaluation of the Blocking Performance. Equation 2 is used to calculate the blocking rate K_r of the mud cake before and after blocking and to evaluate the good or bad blocking performance.

$$K_r = \frac{K - K'}{K} \times 100\% \quad (2)$$

where K_r is the blocking rate, %; K is the permeability before blocking, mD; and K' is the permeability after blocking, mD.

3. RESULTS AND DISCUSSION

3.1. Characterization of the Oil-Based Nanoblocker Poly(MMA–BMA–BA–St).

3.1.1. Infrared Spectrum. Figure 2 shows the infrared spectra of the oil-based nanosealant poly(MMA–BMA–BA–St). As can be seen in Figure 2, the –OH stretching vibration peak of liquid water is indicated at 3461 cm^{−1}, the stretching vibration peak of the benzene ring skeleton and the bending vibration peak of –OH of liquid water at 1635 cm^{−1}, the symmetric variable angle vibration peak of –CH₃ at 1396 cm^{−1}, the antisymmetric stretching vibration peak of C–O–C and the asymmetric stretching

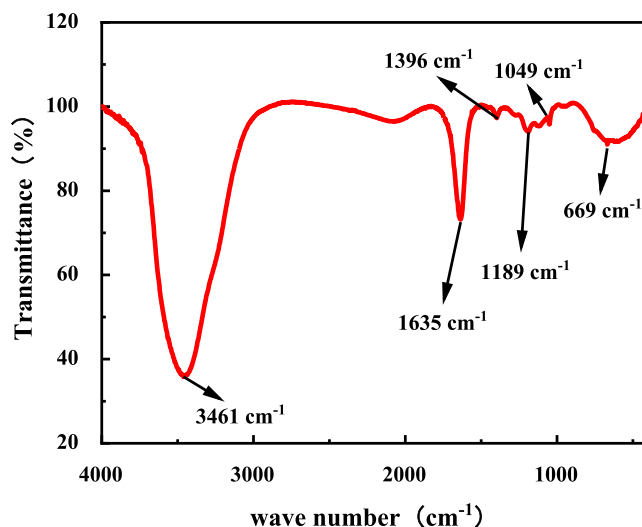


Figure 2. Infrared spectra of poly(VS–St–EMA–BA).

vibration peak of S=O of sulfonate at 1189 cm^{−1}, the symmetric stretching vibration peak of S=O of sulfonate at 1049 cm^{−1}, and the external deformation vibration peak of C–H on the benzene ring at 669 cm^{−1}. The peak of the C=O stretching vibration peak in the ester group is around 1720 cm^{−1}, which is covered by the peak at 1635 cm^{−1}. The functional groups derived from the infrared spectral analysis showed that the quaternary polymer poly(MMA–BMA–BA–St) nanoblocking material was successfully synthesized.

3.1.2. Thermogravimetric Analysis. Figure 3 shows the thermal weight loss analysis curves (TG-DTG curves) of the

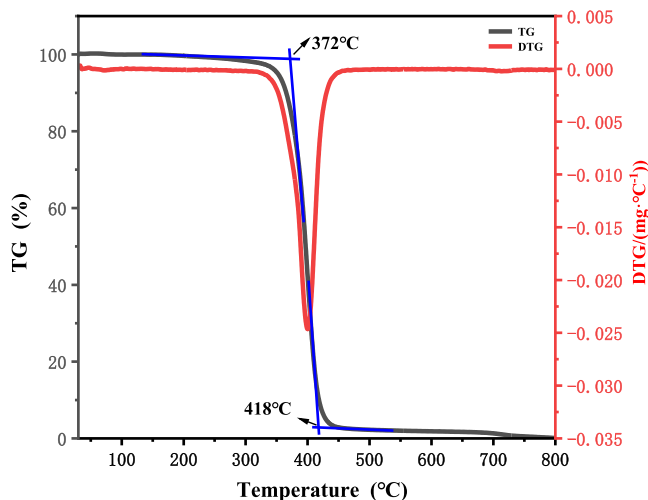


Figure 3. Thermogravimetric analysis of the oil-based nanosealant poly(MMA–BMA–BA–St).

nanoblocker poly(MMA–BMA–BA–St). From the TG-DTG curve in Figure 3, it can be seen that the initial decomposition temperature of the nanoblocker poly(MMA–BMA–BA–St) is 372 °C when the molecular skeleton of poly(MMA–BMA–BA–St) starts to break at high temperature; the final decomposition temperature is 418 °C and the mass loss from 372 to 418 °C is 75.47% when poly(MMA–BMA–BA–St) basically finishes thermal decomposition. The thermogravimetric experimental results illustrate that poly(MMA–BMA–BA–St) can resist the high temperature of 372 °C. The reason

is that the polymer contains a benzene ring with high temperature resistance, which makes poly(MMA–BMA–BA–St) have good temperature resistance, adapt to the high-temperature ground environment, and have good application prospects.²⁸

3.1.3. Grain Size Distribution of Poly(MMA–BMA–BA–St) at Room Temperature. The results of the particle size distribution of the oil-based nanosealer poly(MMA–BMA–BA–St) are shown in Figure 4. The particle size distribution of

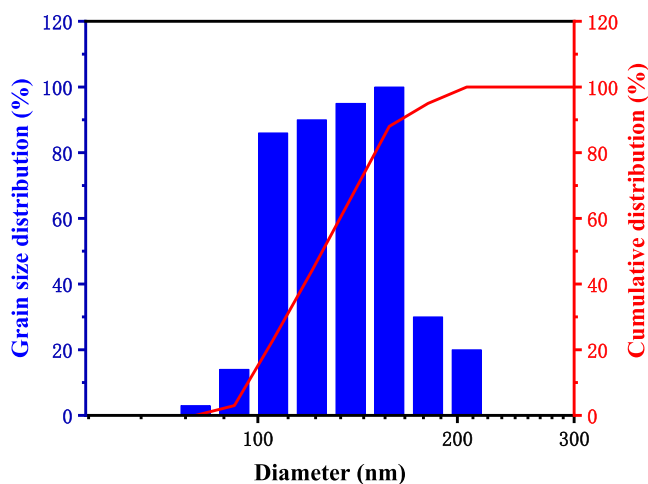


Figure 4. Particle size distribution of the oil-based nanoblocker poly(MMA–BMA–BA–St).

the nanoblocker poly(MMA–BMA–BA–St) can be seen in Figure 4 in the range of 80.56–206.61 nm, with D_{50} of 124.98 nm and D_{90} of 165.79 nm, and the average particle size of 137.10 nm. The particle size of poly(MMA–BMA–BA–St) is nanoscale. For the development of micro and nanofractures in shale formations, poly(MMA–BMA–BA–St) can enter the nanopores or participate in bridging and filling to form a dense sealing layer to achieve effective sealing of micro and nanopores. Poly(MMA–BMA–BA–St) is expected to be effective as an oil-based drilling fluid nanosealant for sealing micro-nanopores in shale formations.

3.2. Drilling Fluid Performance Evaluation. As the addition of a small amount of poly(MMA–BMA–BA–St) can achieve an excellent sealing effect, by adding 0.00, 0.25, 0.50, 0.75, 1.00 wt % of the oil-based nanosealant poly(MMA–BMA–BA–St) to formulate the oil-based drilling fluid, the drilling fluid was tested at 150 °C for the rheological properties, emulsion breaking voltage, and HTHP filtration loss, and the performance parameters are shown in Figures 5–11. As can be seen from Figure 5, the apparent viscosity of oil-based drilling fluid increased with the increase of poly(MMA–BMA–BA–St) addition. The apparent viscosity of the base slurry was 64.0 mPa s, and when the addition amount was 1.00 wt %, the apparent viscosity was 72.5 mPa s, which increased by 13.28% compared with the base slurry. The change was the maximum at this time; the reason is that poly(MMA–BMA–BA–St) can form a continuous and dense spatial mesh structure in water, and as the concentration of poly(MMA–BMA–BA–St) increases, the mesh structure becomes more dense and the width of the mesh skeleton is larger, thus increasing the viscosity of the drilling fluid. As shown in Figure 6, the plastic viscosity of the base slurry was 50.5 mPa s, and the addition of poly(MMA–BMA–BA–St)

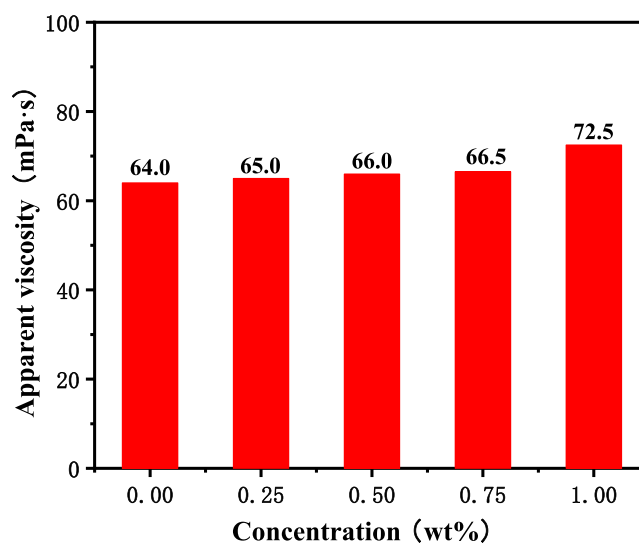


Figure 5. Apparent viscosity change curve of the oil-based drilling fluid with the addition of poly(MMA–BMA–BA–St).

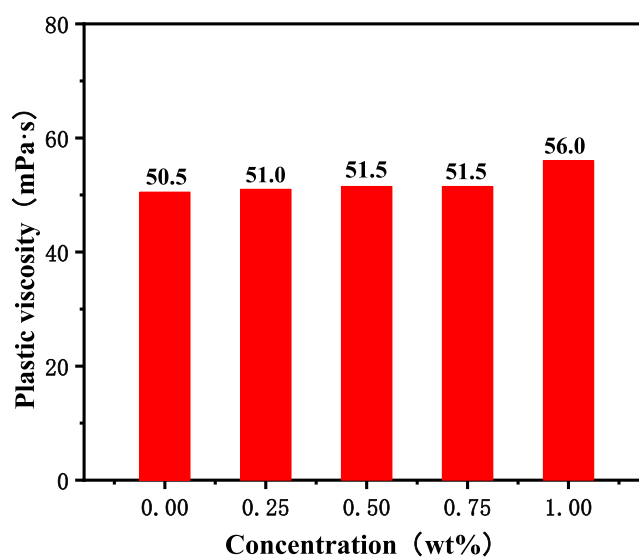


Figure 6. Plastic viscosity change curve of the oil-based drilling fluid with the addition of poly(MMA–BMA–BA–St).

increased the plastic viscosity of the oil-based drilling fluid to 56.0 mPa s when the addition amount was 1.00 wt %, which increased 10.89% compared to the base slurry. As shown in Figure 7, the dynamic shear of the oil-based drilling fluid with the addition of poly(MMA–BMA–BA–St) was maintained at 13.5–16.5 Pa, which increased with the addition amount; the reason for this is that the dense spatial mesh structure increases the viscosity of the drilling fluid, which in turn increases the dynamic shear of the drilling fluid. From Figure 8, it can be seen that the dynamic-plastic ratio of the oil-based drilling fluid with the addition of poly(MMA–BMA–BA–St) increases with the increase of poly(MMA–BMA–BA–St); the dynamic shear force of the drilling fluid increases substantially, thus improving the dynamic-plastic ratio of the drilling fluid, and the dynamic-plastic ratio is maintained between 0.27 and 0.29, at which time the drilling fluid has a better rock-carrying ability and borehole cleaning ability. As can be seen from Figure 9, poly(MMA–BMA–BA–St) has less influence on the breaking voltage of the drilling fluid, and the breaking voltage is

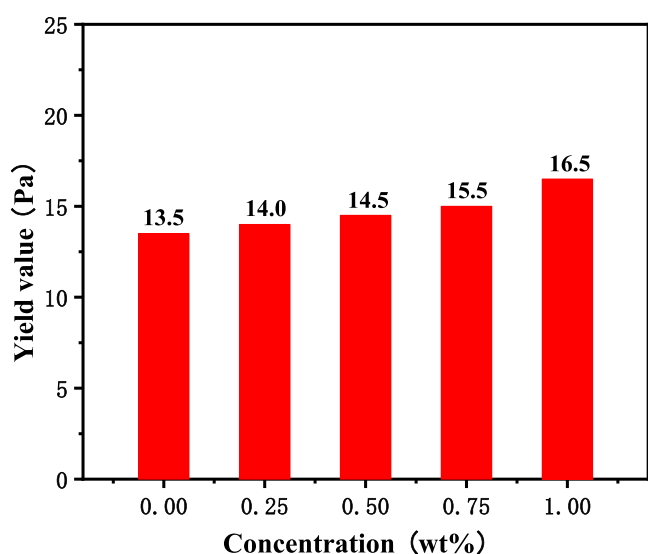


Figure 7. Yield value change curve of the oil-based drilling fluid with the addition of poly(MMA-BMA-BA-St).

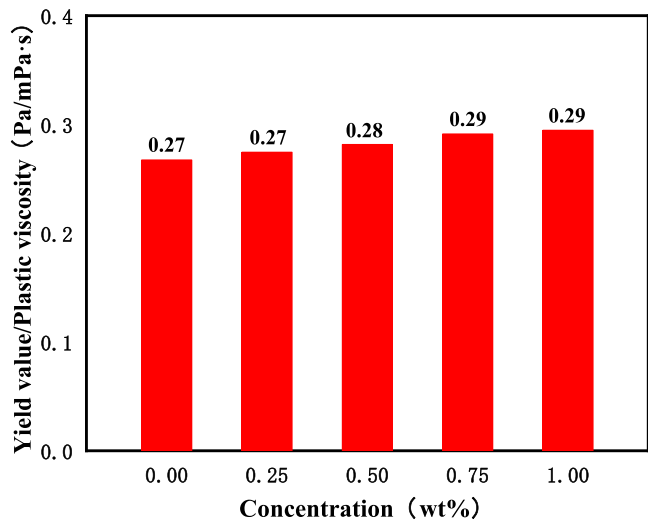


Figure 8. Variation curve of yield value/plastic viscosity of the oil-based drilling fluid with the addition of poly(MMA-BMA-BA-St).

maintained above 600 V. The drilling fluid shows better stability. The test results in Figures 5–9 show that poly(MMA-BMA-BA-St) has less effect on the rheology and electrical stability of the oil-based drilling fluid, and poly(MMA-BMA-BA-St) has better compatibility with the oil-based drilling fluid. As shown in Figure 10, when poly(MMA-BMA-BA-St) was added at 0.50 wt %, the HTHP filtration loss was 2.2 mL, which was 26.7% lower compared to the base slurry filtration loss, indicating that poly(MMA-BMA-BA-St) played a plugging role in the oil-based drilling fluid. Figure 11 shows the HTHP experimental mud cake of the oil-based drilling fluid with the addition of poly(MMA-BMA-BA-St). Poly(MMA-BMA-BA-St) has good dispersion in the oil-based drilling fluid and forms a smoother blocking layer. The performance of the oil-based drilling fluid with the addition of poly(MMA-BMA-BA-St) is more stable, and the influence of filtrate intrusion on the formation is reduced. Poly(MMA-BMA-BA-St) can be applied in the oil-based drilling fluid.

3.3. Evaluation of the Blocking Performance. Table 1 shows the mud cake permeability results for different additions

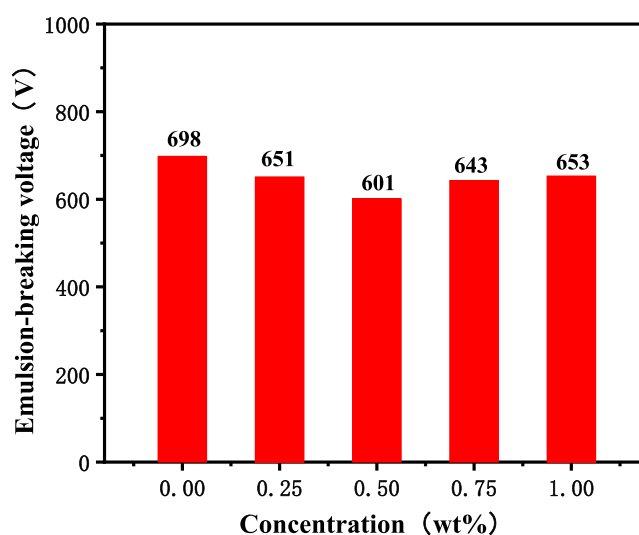


Figure 9. Change curve of the breaking voltage of the oil-based drilling fluid with the addition of poly(MMA-BMA-BA-St).

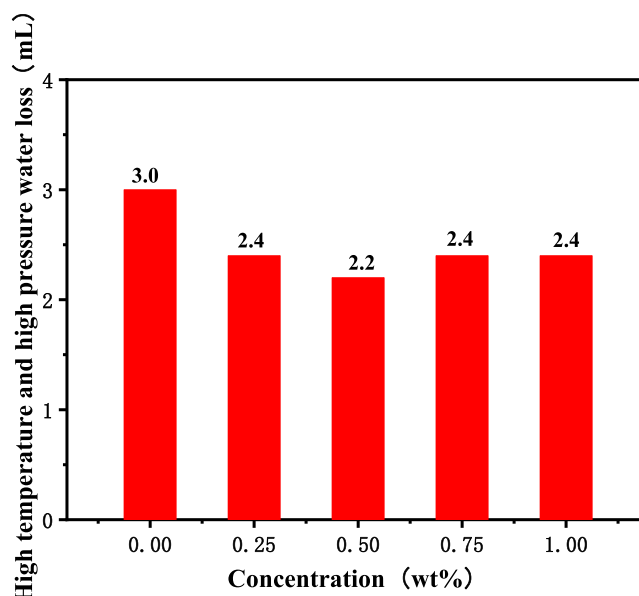


Figure 10. HTHP variation curve of the oil-based drilling fluid with the addition of poly(MMA-BMA-BA-St).

of the oil-based nanosealer poly(MMA-BMA-BA-St). It can be seen from Table 1 that with the increase of poly(MMA-BMA-BA-St) addition, the filtration loss decreased from 3.0 to 2.2 mL and the sludge cake thickness changed less. When poly(MMA-BMA-BA-St) was 0.50 wt %, the mud cake permeability was the smallest (1.12×10^{-4} mD), and the permeability was reduced by 30.00% compared to the oil-based drilling fluid without the added plugging agent. Table 2 shows the artificial core permeability of the oil-based drilling fluid with the addition of the 0.50 wt % nanosealer poly(MMA-BMA-BA-St). As can be seen from Table 2, the white oil permeability of poly(MMA-BMA-BA-St) with the addition of 0.50 wt % nanoblocker is 4.05×10^{-4} mD, which is 91.23% lower than that of pure white oil, and the plugging rate is higher than that of similar nanoblockers.²⁹ The mud cake permeability and artificial core permeability results show that poly(MMA-BMA-BA-St) has good plugging performance

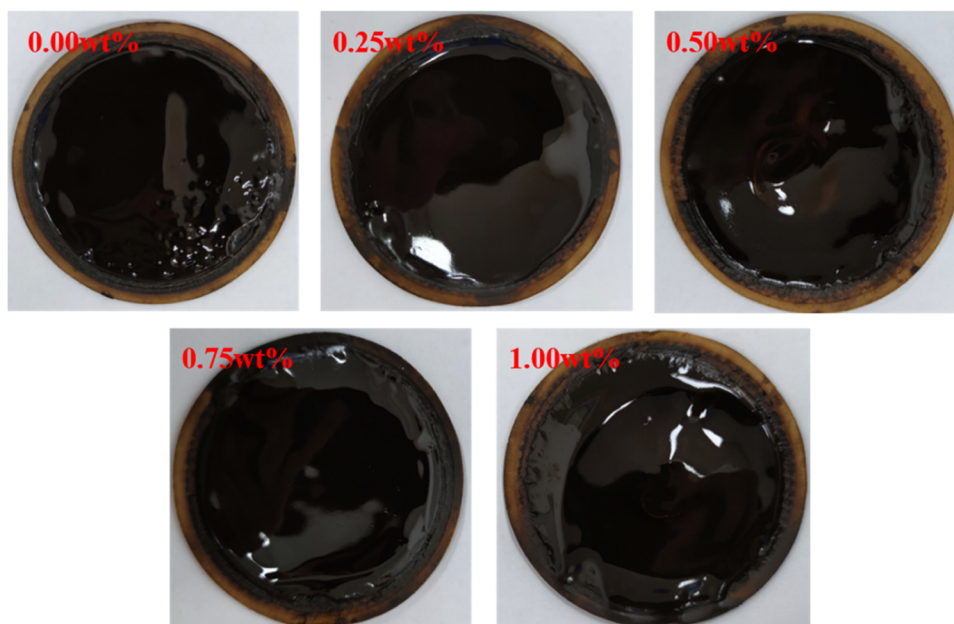


Figure 11. HTHP mud cake after blocking with the oil-based nanoblocking agent poly(MMA-BMA-BA-St).

Table 1. Permeability of the Oil-Based Drilling Fluid Mud Cake with the Addition of the Oil-Based Nanosealant Poly(MMA-BMA-BA-St)

concentration, wt %	filtration loss, mL	thickness of mud cake, cm	K_f , 10^{-4} mD	K'_f , 10^{-4} mD	K_r , %
0.00	3.00	0.20	1.60		0.00
0.25	2.40	0.18		1.15	28.13
0.50	2.20	0.19		1.12	30.00
0.75	2.40	0.21		1.34	16.25
1.00	2.40	0.20		1.28	20.00

Table 2. Permeability of Artificial Cores of Oil-Based Drilling Fluids with the 0.50 wt % Oil-Based Nanosealer Poly(MMA-BMA-BA-St)

	concentration, wt %	permeability after blocking, 10^{-3} mD	K_r , %
poly(MMA-BMA-BA-St)	0.00	4.56	
	0.50	0.40	91.23
poly(AM-co-AA)/SiO ₂ ²⁹	0.00	2.17	
		0.35	83.87
poly(AM-co-AA) ²⁹	0.00	2.06	
		0.57	72.23

and can be used as an effective nanoplugging agent in oil-based drilling fluids.

3.4. Nanoblocking Mechanism Research. Figure 12 shows the sealing mechanism of the oil-based nanosealing material poly(MMA-BMA-BA-St) by the HTHP filter loss experiment, mud cake, and artificial core permeability results. Combined with the particle size distribution of the oil-based nanoplugging agent poly(MMA-BMA-BA-St), it can be seen that the conventional micron-plugging materials cannot enter the nanopore joints and tend to accumulate outside the nanofractures; however, this accumulation layer is easily destroyed in the drilling fluid circulation and cannot stop the intrusion of the drilling fluid, which leads to well wall destabilization. At the same time, poly(MMA-BMA-BA-

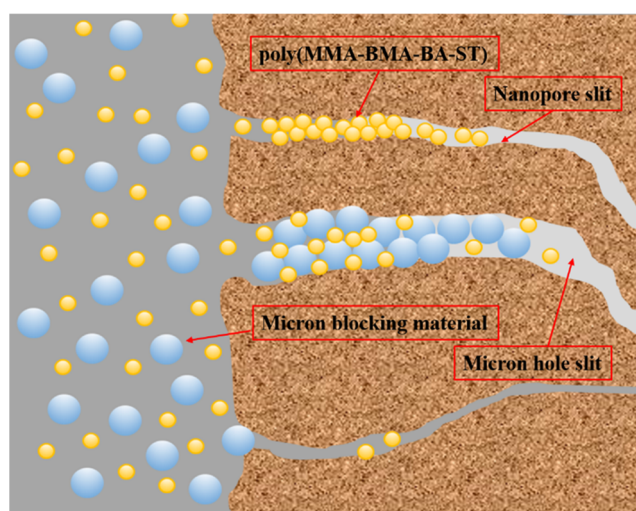


Figure 12. Blocking mechanism of the oil-based nanoblocker poly(MMA-BMA-BA-St).

St) can also be used in combination with large-size ($>1 \mu\text{m}$) rigid plugging materials to fill nanopores, making the plugging layer more dense, thus playing a role in reducing the amount of filtration loss and reducing filtrate intrusion into the formation.³⁰

4. CONCLUSIONS

- (1) The oil-based nanosealant poly(MMA-BMA-BA-St) was synthesized by the Michael addition reaction using compounds such as styrene, methyl methacrylate, and butyl methacrylate. Poly(MMA-BMA-BA-St) is resistant to the high temperature of 372 °C, has a particle size distribution between 80.56 and 206.61 nm with an average particle size of 137.10 nm, and can seal nanosized pores.
- (2) The oil-based nanosealant poly(MMA-BMA-BA-St) has less effect on the apparent viscosity, plastic viscosity,

and yield value oil-based drilling fluid performance, with a kinetic-plastic ratio higher than 0.27 and breaking voltage higher than 600 V. The overall performance parameters change less, and the drilling fluid has excellent rock-carrying performance and wellbore purification performance. With the addition of poly-(MMA–BMA–BA–St), the filtration loss of the oil-based drilling fluid decreased and the mud cake became smooth. HTHP with 0.50 wt % addition had the lowest filtration loss, corresponding to a mud cake permeability of 1.12×10^{-4} mD and a blocking rate was 30.00%; the permeability of the artificial core was 4.0×10^{-4} mD, and the blocking rate was 91.23%.

- (3) The oil-based nanoplugging agent poly(MMA–BMA–BA–St), as a nanoplugging material, can effectively seal nanopores and seams or be used in combination with large-size plugging materials to reduce the influence of the filtrate on the formation, thus playing a role in maintaining well wall stability and reducing downhole complications. The oil-based nanoplugging agent poly-(MMA–BMA–BA–St) has good application prospects.

AUTHOR INFORMATION

Corresponding Author

Gang Xie – State Key Laboratory of Oil & Gas Reservoir Geology and Exploitation, Southwest Petroleum University, Chengdu 610500 Sichuan, China; orcid.org/0000-0002-1608-1103; Email: 201899010129@swpu.edu.cn

Authors

Daqi Li – State Key Laboratory of Shale Oil and Gas Enrichment Mechanisms and Effective Development, Sinopec Research Institute of Petroleum Engineering, Beijing 102206, China

Xianguang Wang – State Key Laboratory of Shale Oil and Gas Enrichment Mechanisms and Effective Development, Sinopec Research Institute of Petroleum Engineering, Beijing 102206, China

Yu Chen – State Key Laboratory of Oil & Gas Reservoir Geology and Exploitation, Southwest Petroleum University, Chengdu 610500 Sichuan, China

Zixuan Han – State Key Laboratory of Shale Oil and Gas Enrichment Mechanisms and Effective Development, Sinopec Research Institute of Petroleum Engineering, Beijing 102206, China

Complete contact information is available at:
<https://pubs.acs.org/10.1021/acsomega.2c03164>

Notes

The authors declare no competing financial interest.

ACKNOWLEDGMENTS

This work was financially supported by the Joint Enterprise Innovation and Development Fund Integrated Project: Fundamental Research on Offshore Deep Oil and Gas Enrichment Mechanisms and Key Engineering Technologies Basic Research Program on Deep Petroleum Resource Accumulation and Key Engineering Technologies (U19B6003).

REFERENCES

- (1) Chen, T.-Y.; Feng, X.-T.; Cui, G.-L.; Tan, Y.-L.; Pan, Z.-J. Experimental study of permeability change of organic-rich gas shales under high effective stress. *J. Nat. Gas Sci. Eng.* **2019**, *64*, 1–14.
- (2) Huang, H.-X.; Sun, W.; Xiong, F.-Y.; Chen, L.; Li, X.; Gao, T.; Jiang, Z.-X.; Ji, W.; Wu, Y.-J.; Han, J. A novel method to estimate subsurface shale gas capacities. *Fuel* **2018**, *232*, 341–350.
- (3) Cui, H.-Y.; Liang, F.; Ma, C.; Zhong, N.-N.; Sha, Y.-L.; Ma, W. Pore evolution characteristics of Chinese marine shale in the thermal simulation experiment and the enlightenment for gas shale evaluation in South China. *Geosci. J.* **2019**, *23*, 595–602.
- (4) Li, J.; Wang, X.; Hou, L.-H.; Chen, C.; Guo, J.-Y.; Yang, C.-L.; Wang, Y.-F.; Li, Z.-S.; Cui, H.-Y.; Hao, A.-S.; Zhang, L. Geochemical characteristics and resource potential of shale gas in Sichuan Basin, China. *J. Nat. Gas Geosci.* **2021**, *6*, 313–327.
- (5) Jia, L.-C.; Tang, G.; Liu, D.-C.; Shi, X. Experimental study the viscoelastic properties of deep shale gas reservoirs in Sichuan Basin. *IOP Conf. Ser.: Earth Environ. Sci.* **2021**, *861*, 062069.
- (6) Tang, L.; Song, Y.; Li, Q.-W.; Paang, X.-Q.; Jiang, Z.-X.; Li, Z.; Tang, X.-L.; Yu, H.-L.; Sun, Y.-Y.; Fan, S.-C.; Zhu, L. A Quantitative Evaluation of Shale Gas Content in Different Occurrence States of the Longmaxi Formation: A New Insight from Well JY-A in the Fuling Shale Gas Field, Sichuan Basin. *Acta Geol. Sin.* **2019**, *93*, 400–419.
- (7) He, S.; Li, S.; Qin, Q.; Long, S.-X. Influence of Mineral Compositions on Shale Pore Development of Longmaxi Formation in the Dingshan Area, Southeastern Sichuan Basin, China. *Energy Fuels* **2021**, *35*, 10551–10561.
- (8) Yan, X.-P.; Kang, Y.-L.; You, L.-J.; Xu, C.-Y.; Lin, C.; Zhang, J.-Y. Drill-in fluid loss mechanisms in brittle gas shale: A case study in the Longmaxi Formation, Sichuan Basin, China. *J. Pet. Sci. Eng.* **2019**, *174*, 394–405.
- (9) Murtaza, M.; Sulaiman, A.-A.; Muhammad, S.-K.; Sagheer, A.-O.; Mohammed, A.; Mohamed, M. Experimental Investigation of the Rheological Behavior of an Oil-Based Drilling Fluid with Rheology Modifier and Oil Wetter Additives. *Molecules* **2021**, *26*, 4877.
- (10) Murtaza, M.; Hafiz, M.-A.; Muhammad, S.-K.; Syed, S.-H.; Mohamed, M.; Shirish, P. Evaluation of Clay Hydration and Swelling Inhibition Using Quaternary Ammonium Dicationic Surfactant with Phenyl Linker. *Molecules* **2020**, *25*, 4333.
- (11) Wang, B.; Li, W.; Zhang, W.; Li, H.; Wang, T. Performance Optimization of a Water Base Drilling Fluid for Continental Shale Gas Drilling in Block Yanchang. *Drill. Fluid Completion Fluid* **2018**, *35*, 74–78.
- (12) Wang, B.-J.; Luo, C.-Z.; Wang, Y.-D. Research and Application of Fuling Shale Gas Anti-Collapse and Anti-Leakage Drilling Fluid System. *Open J. Yangtze Oil Gas* **2021**, *06*, 60–71.
- (13) Wu, L. Enhancing Pressure Bearing Capacity of Formation to Control Mud Losses in Deep Shale Gas Drilling With Oil Base Drilling Fluids. *Zuanjingye Wanjingye* **2018**, *35*, 37–41.
- (14) Peng, B.-Q.; Zhou, F.; Li, M.-S.; Zhang, J.-L. Optimization and Evaluation of Anti-collapse Water-based Drilling Fluids for Shale Gas Horizontal Wells: A Case Study of the Changning-Weiyuan National Shale Gas Demonstration Area. *Nat. Gas Ind.* **2017**, *37*, 89–94.
- (15) Guo, H.; Voncken, J.; Opstal, T.; Dams, R.; Zitha, L.-J. Investigation of the Mitigation of Lost Circulation in Oil-Based Drilling Fluids by Use of Gilsonite. *SPE J.* **2014**, *19*, 1184–1191.
- (16) Wang, B.; Sun, J.-S.; Shen, F.; Li, W.; Zhang, W.-Z. Mechanism of wellbore instability in continental shale gas horizontal sections and its water-based drilling fluid countermeasures. *Nat. Gas Ind. B* **2020**, *7*, 680–688.
- (17) Kerunwa, A.; Ekwueme, S.-T. An Approach to Curbing Wellbore Instability in Shales through Nanoparticles- Augmented Water-Based Drilling Muds. *Pet. Coal* **2020**, *62*, 1465–1473.
- (18) Yan, X.-P.; Kang, Y.-L.; You, L.-J. Wellbore Instability Induced by the Coupling of High-pH Fluid–Shale Reaction and Fracture Surface Sliding in Shale Gas Wells: Experimental and Field Studies. *Energy Fuels* **2020**, *34*, 5578–5588.

- (19) Tan, Q.; Yu, B.-H.; Deng, J.-E.; Zhao, K.; Chen, J.-G. Study on wellbore stability and instability mechanism in Piedmont structures. *Open Pet. Eng. J.* **2015**, *8*, 208–213.
- (20) Xie, G.; Luo, P.-Y.; Deng, M.-Y.; Wang, Z.; Gong, R. Hyperbranched polyamine as nano-plugging agent used in water-based drilling fluid. *Nanosci. Nanotechnol. Lett.* **2017**, *9*, 310–315.
- (21) Liu, F.; Zheng, Z.; Wang, X.-Y.; Li, X.-Q.; Zhang, Z.; Wang, X.-W.; Dai, X.-D.; Xin, Y.-P.; Liu, Q.-X.; Yao, H.-L.; Jiang, S.-Y.; Liu, C.; Li, X.-Y. Novel modified nano-silica/polymer composite in water-based drilling fluids to plug shale pores. *Energy Sources* **2021**, *16*, 1893044.
- (22) Xie, G.; Luo, P.-Y.; Deng, M.-Y.; Wang, Z. Nanoplugging Performance of Hyperbranched Polyamine as Nanoplugging Agent in Oil-Based Drilling Fluid. *J. Nanomater.* **2015**, *2015*, 821910.
- (23) Geng, Y.; Sun, J.-S.; Wang, J.-H.; Wang, R.; Yang, J.; Wang, Q.-B.; Ni, X.-X. Modified Nanopolystyrene as a Plugging Agent for Oil-Based Drilling Fluids Applied in Shale Formation. *Energy Fuels* **2021**, *35*, 16543–16552.
- (24) Li, W.-Q.; Jiang, G.-C.; Ni, X.-X.; Li, Y.-Y.; Wang, X.-Z.; Luo, X.-G. Styrene butadiene resin/nano-SiO₂ composite as a water-and-oil-dispersible plugging agent for oil-based drilling fluid. *Colloids Surf., A* **2020**, *606*, No. 125245.
- (25) Li, H.; Kaihe, L.; Xianbin, H.; Zhen, L.; Xiaodong, D. The Synthesis of Polymeric Nanospheres and the Application as High-Temperature Nano-Plugging Agent in Water Based Drilling Fluid. *Front. Chem.* **2020**, *8*, 247.
- (26) Li, P. Preparation of a novel nano polymer emulsion plugging agent using in drilling fluids for shale gas exploration. *Fresenius Environ. Bull.* **2020**, *29*, 1798–1803.
- (27) Naga, N.; Satoh, M.; Magara, T.; Ahmed, K.; Nakano, T. Synthesis of porous polymers by means of Michael addition reaction of multifunctional acetoacetate and poly(ethylene glycol) diacrylate. *Eur. Polym. J.* **2022**, *162*, No. 110901.
- (28) Zhang, Y.; Mao, J.; Zhao, J.; Zhang, W.; Liao, Z.; Xu, T.; Du, A.; Zhang, Z.; Yang, X.; Ni, Y. Preparation of a novel sulfonic Gemini zwitterionic viscoelastic surfactant with superior heat and salt resistance using a rigid-soft combined strategy. *J. Mol. Liq.* **2020**, *318*, No. 114057.
- (29) Tang, X. C.; Yang, H. B.; Gao, Y. B.; Lashari, Z. A.; Cao, C. X.; Kang, W. L. Preparation of a micron-size silica-reinforced polymer microsphere and evaluation of its properties as a plugging agent. *Colloids Surf., A* **2018**, *547*, 8–18.
- (30) Jia, J.; Zhao, D.; Chen, H. Study on properties and mechanism of nano-blocking agent for water-based drilling fluids. *Fresenius Environ. Bull.* **2020**, *29*, 43–50.